

1 **Supplementary information, Data S1**

2 **Methods and Materials**

3 **Cloning**

4 The human $\alpha 5$ and $\beta 3$ GABA_A receptor genes (NCBI Reference Sequence:
5 NM_000810.3 and NM_000814.5) were cloned into pEGBacMam vector containing
6 either His₁₀-tag or Twin-Strep-tag at the C-terminus. Deletion constructs used for
7 expression and structural analysis lack a large portion of the intracellular loop
8 connecting TM3 and TM4. Residues from Arg347 to Ser423 in the $\alpha 5$ subunit, and that
9 from Gly333 to Asn446 in the $\beta 3$ subunit, were replaced with the short amino acid
10 sequence SQPARAA, as previously described ^{1,2}.

11

12 **Expression and purification**

13 The bacmids and baculoviruses were generated using standard methods. The P2 viruses
14 of the same MOIs for the $\alpha 5$ and $\beta 3$ subunits were used to infect HEK293S-GnTI⁻ cell
15 at 37 °C with 10 mM sodium butyrate. Cells were collected after ~72h post-infection
16 by centrifugation, resuspended in buffer A (20 mM HEPES-NaOH, pH 7.4, 300 mM
17 NaCl), and disrupted by sonication. The membranes were pelleted from the supernatant
18 by centrifugation for 1 h at 48000g. Membrane pellets were mechanically homogenized
19 and solubilized in buffer A supplemented with 1% (w/v) lauryl maltose neopentyl
20 glycol (LMNG, Anatrace) and 0.1% (w/v) cholesteryl hemisuccinate (CHS, Sigma
21 Aldrich), and by gentle agitation for 3 h on ice. Non-solubilized material was removed
22 by ultracentrifugation (48000g and 40 min). The supernatant was incubated with Strep-

23 Tactin Sepharose (IBA Lifesciences) for 1 h with gentle rotation at 4°C. The resin was
24 washed in buffer B (buffer A+0.006% LMNG+0.0006% CHS) and eluted in the same
25 buffer containing 10 mM D-desthiobiotin (Sigma-Aldrich). The protein was further
26 loaded onto a column containing 1 ml of the Co²⁺ affinity resin and eluted by 250 mM
27 imidazole in buffer B. The nanobody Nb25, expressed and purified as described below,
28 was added to the heteromeric $\alpha 5\beta 3$ GABA_A receptor at ten-fold molar excess and the
29 complex were further purified by size-exclusion chromatography (SEC) in buffer C (20
30 mM HEPES-NaOH, pH 7.4, 100 mM NaCl, 0.006% LMNG and 0.0006% CHS, 1 mM
31 GABA). Fractions containing the receptor were pooled and concentrated to 2mg/ml.

32

33 **Nanobody purification**

34 The nanobody Nb25, was cloned into plasmid pET21a with an N-terminal PelB signal
35 peptide and a C-terminal His₆-tag. The protein was expressed and purified from *E. coli*.
36 Cultures were grown at 37 °C until their OD₆₀₀ reached 0.6-0.8, at which point
37 expression was induced with 1 mM IPTG. After induction, cells were grown at 28 °C
38 overnight and harvested by centrifugation (20 min, 4,000 g). Nanobodies were released
39 from the bacterial periplasm, purified using nickel affinity chromatography, and then
40 subjected to size-exclusion chromatography on a Superdex 75 16/600 column (GE
41 Healthcare) in buffer A.

42

43 **Cryo-EM Sample preparation**

44 2.5 µl samples of purified protein were applied to glow-discharged holey carbon grids

45 (Quantifoil R1.2/1.3 Au 200 mesh). Excess liquid was removed in a controlled
46 environment (4 °C and 100% relative humidity) by blotting grids for 3s (with a blotting
47 force of -15), then plunge-frozen into liquid ethane cooled by liquid nitrogen using a
48 Vitrobot Mark IV (FEI).

49 **Cryo-EM image collection and processing**

50 CryoEM images were recorded on a Gatan K2 Summit direct electron detector in an
51 FEI Titan Krios electron microscope (FEI) equipped with GIF quantum energy filter
52 (Gatan) operated at 300 kV. Legion³ was used to semi-automatically record zero
53 energy-loss (20 eV slit) image frames at a nominal magnification of 130,000 x
54 (calibrated pixel size: 1.07Å/pixel on the sample) in counting mode. Images were
55 recorded as movies consisting of 40 frames with total dose of 56 e-/Å² and an exposure
56 of 8s. Preset defocus values ranged from 1.4 to 2 μm.

57 Individual movie frames were aligned, dose-weighted and summed using MotionCor2
58⁴. Defocus and astigmatism parameters were estimated using Gctf⁵. Particle picking
59 was performed in Gautomatch using projections from low pass filtered structure
60 previously collected in-house. Total 699,673 particles were extracted from 3,724
61 micrographs using Relion 2.1⁶. All subsequent image processing was carried out in
62 cryoSPARC⁷. A set of 434,120 particles after 2D classification was selected to perform
63 downstream image processing. 4 previous determined GABA_A receptor structures with
64 different number of nanobodies were used as initial models in the Heterogeneous
65 refinement in cryoSparc. A set with the highest reported resolution was chosen and total
66 161,455 particles were subject to the final 3D refinement in cryoSPARC (Figure S5).

67 The final model was refined to an overall resolution of 3.51 Å (Figure S6). This model
68 and the map sharpened by LocScale⁸ were used for model building.

69 **Model building and refinement**

70 The atomic models of human GABA_A receptor (PDB ID: 4COF)¹, and nanobody model
71 (PDB ID: 5O8F)² and a homology model of $\alpha 5$ subunit generated by submitting the
72 sequence to the swiss-model website⁹ were fitted into the 3D density maps using UCSF
73 Chimera¹⁰ and used as initial models for atomic model building. Individual amino acid
74 residues of each initial model were then manually adjusted in Coot¹¹, guided by well
75 resolved features of side chain densities. Models were optimized with Phenix¹² and re-
76 adjusted in Coot, iteratively, until no further improvement in model geometry could be
77 obtained.

78

79 **Reference:**

- 80 1 Miller, P. S. & Aricescu, A. R. Crystal structure of a human GABAA receptor. *Nature* **512**,
81 270-275, doi:10.1038/nature13293 (2014).
- 82 2 Miller, P. S. *et al.* Structural basis for GABAA receptor potentiation by neurosteroids. *Nat*
83 *Struct Mol Biol* **24**, 986-992, doi:10.1038/nsmb.3484 (2017).
- 84 3 Suloway, C. *et al.* Fully automated, sequential tilt-series acquisition with Leginon. *J Struct*
85 *Biol* **167**, 11-18, doi:10.1016/j.jsb.2009.03.019 (2009).
- 86 4 Zheng, S. Q. *et al.* MotionCor2: anisotropic correction of beam-induced motion for
87 improved cryo-electron microscopy. *Nat Methods* **14**, 331-332, doi:10.1038/nmeth.4193
88 (2017).
- 89 5 Zhang, K. Gctf: Real-time CTF determination and correction. *J Struct Biol* **193**, 1-12,
90 doi:10.1016/j.jsb.2015.11.003 (2016).
- 91 6 Kimanius, D., Forsberg, B. O., Scheres, S. H. & Lindahl, E. Accelerated cryo-EM structure
92 determination with parallelisation using GPUs in RELION-2. *Elife* **5**,
93 doi:10.7554/eLife.18722 (2016).
- 94 7 Punjani, A., Rubinstein, J. L., Fleet, D. J. & Brubaker, M. A. cryoSPARC: algorithms for rapid
95 unsupervised cryo-EM structure determination. *Nat Methods* **14**, 290-296,
96 doi:10.1038/nmeth.4169 (2017).
- 97 8 Jakobi, A. J., Wilmanns, M. & Sachse, C. Model-based local density sharpening of cryo-
98 EM maps. *Elife* **6**, doi:10.7554/eLife.27131 (2017).
- 99 9 Waterhouse, A. *et al.* SWISS-MODEL: homology modelling of protein structures and

100 complexes. *Nucleic Acids Res*, doi:10.1093/nar/gky427 (2018).

101 10 Pettersen, E. F. *et al.* UCSF Chimera--a visualization system for exploratory research and
102 analysis. *J Comput Chem* **25**, 1605-1612, doi:10.1002/jcc.20084 (2004).

103 11 Emsley, P. & Cowtan, K. Coot: model-building tools for molecular graphics. *Acta*
104 *Crystallogr D Biol Crystallogr* **60**, 2126-2132, doi:10.1107/S0907444904019158 (2004).

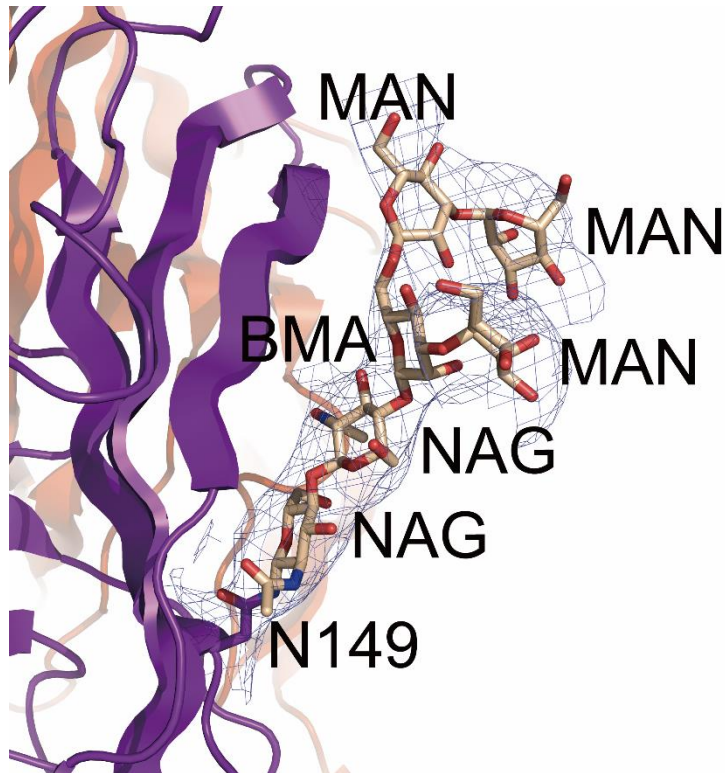
105 12 Afonine, P. V. *et al.* Towards automated crystallographic structure refinement with
106 phenix.refine. *Acta Crystallogr D Biol Crystallogr* **68**, 352-367,
107 doi:10.1107/S0907444912001308 (2012).

108

109

110 Supplementary Table and Figures:

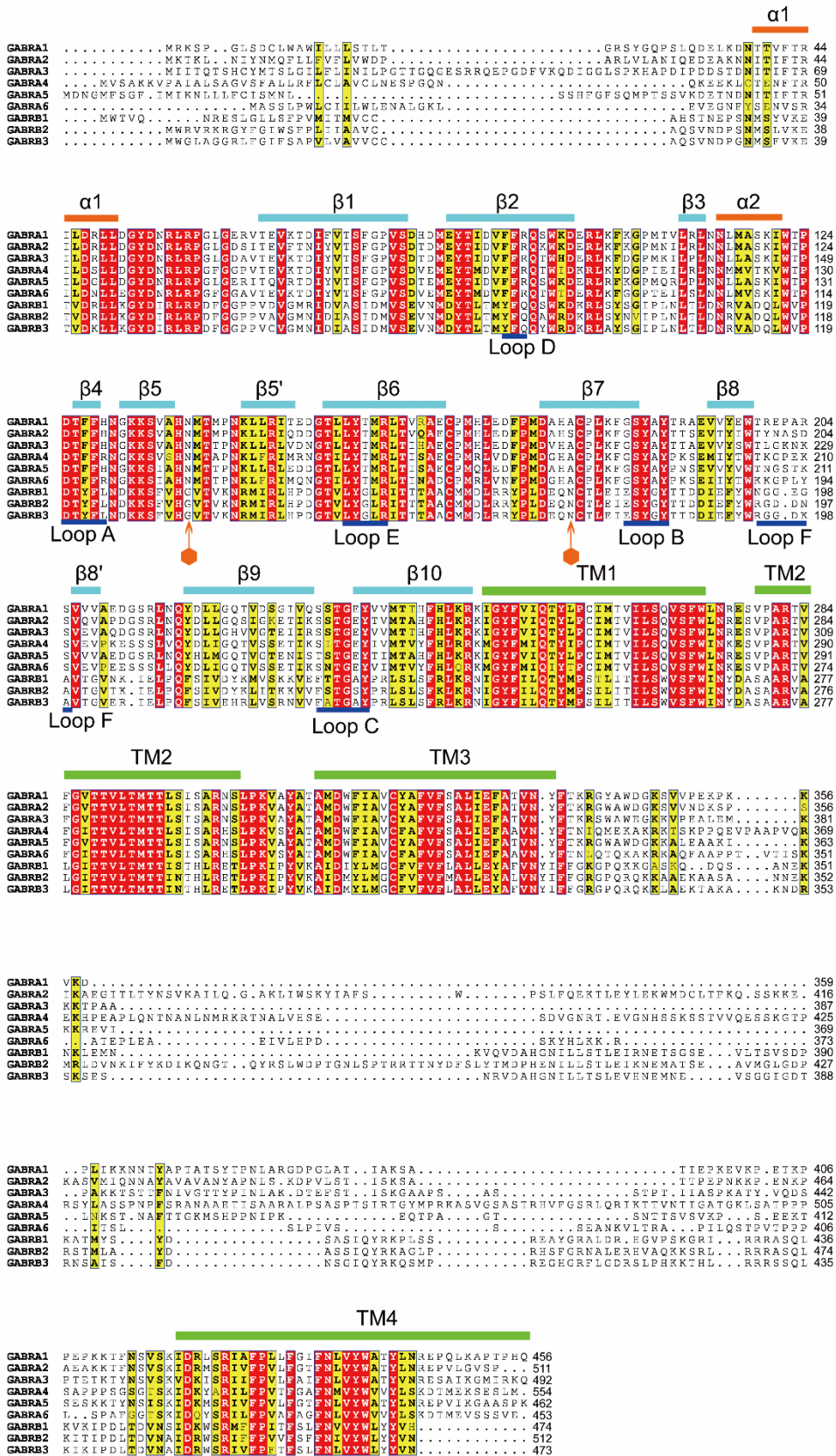
111



112

113 Figure S1. Cryo-EM map at 3σ contour level showing the N-linked glycan at Asn 149
114 of β subunit.

115

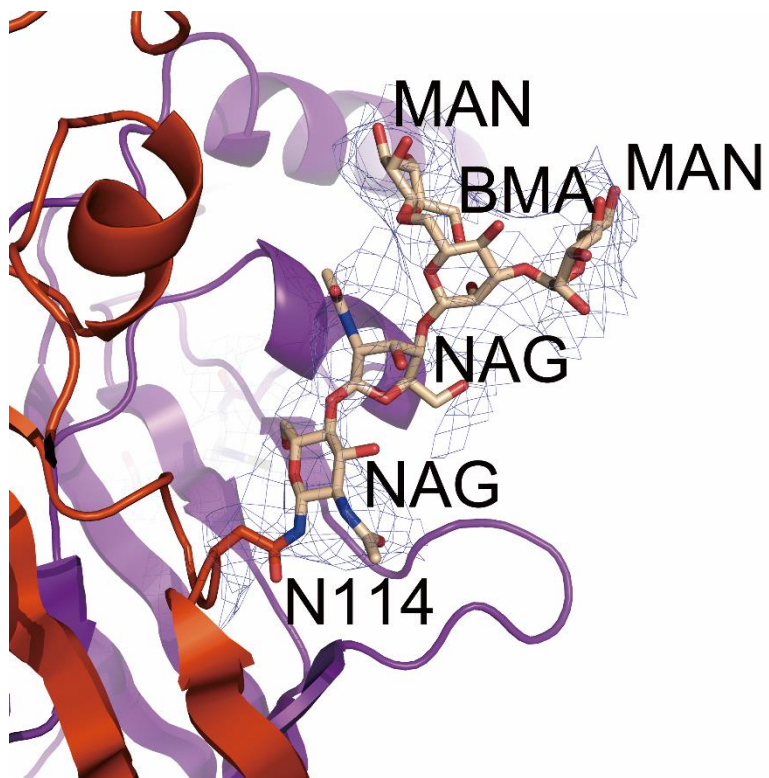


116

117 Figure S2. Sequence alignment of all α and β subunits of human GABA_A receptor.

118 Secondary structure elements were labeled.

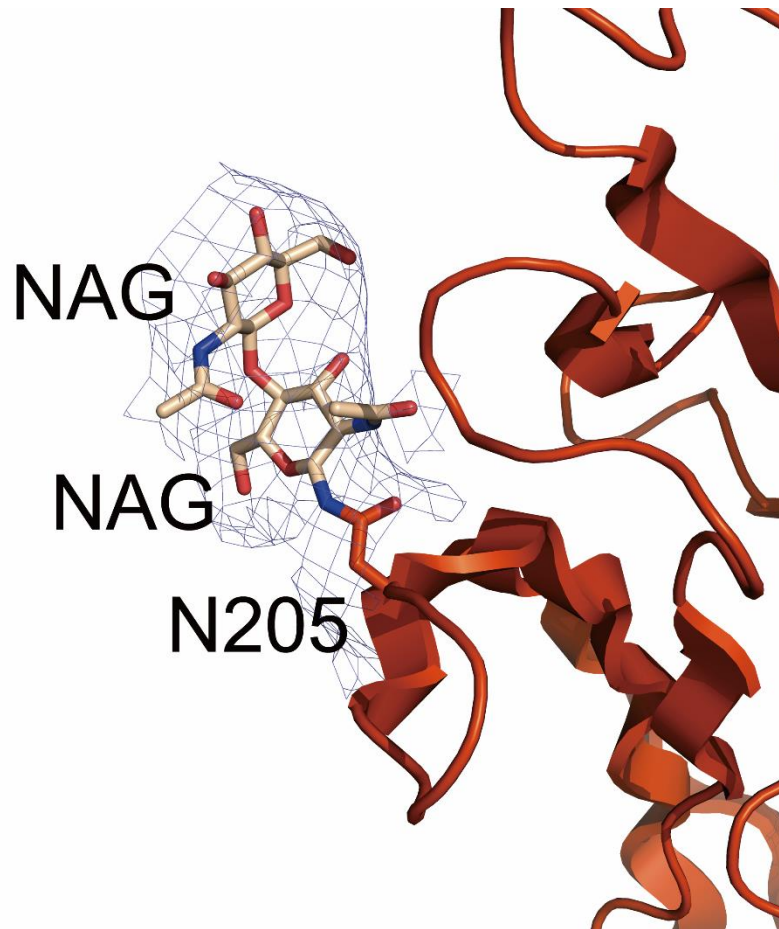
119



120

121 Figure S3. Cryo-EM map at 3σ contour level showing the N-linked glycan at Asn 114
122 of α subunit.

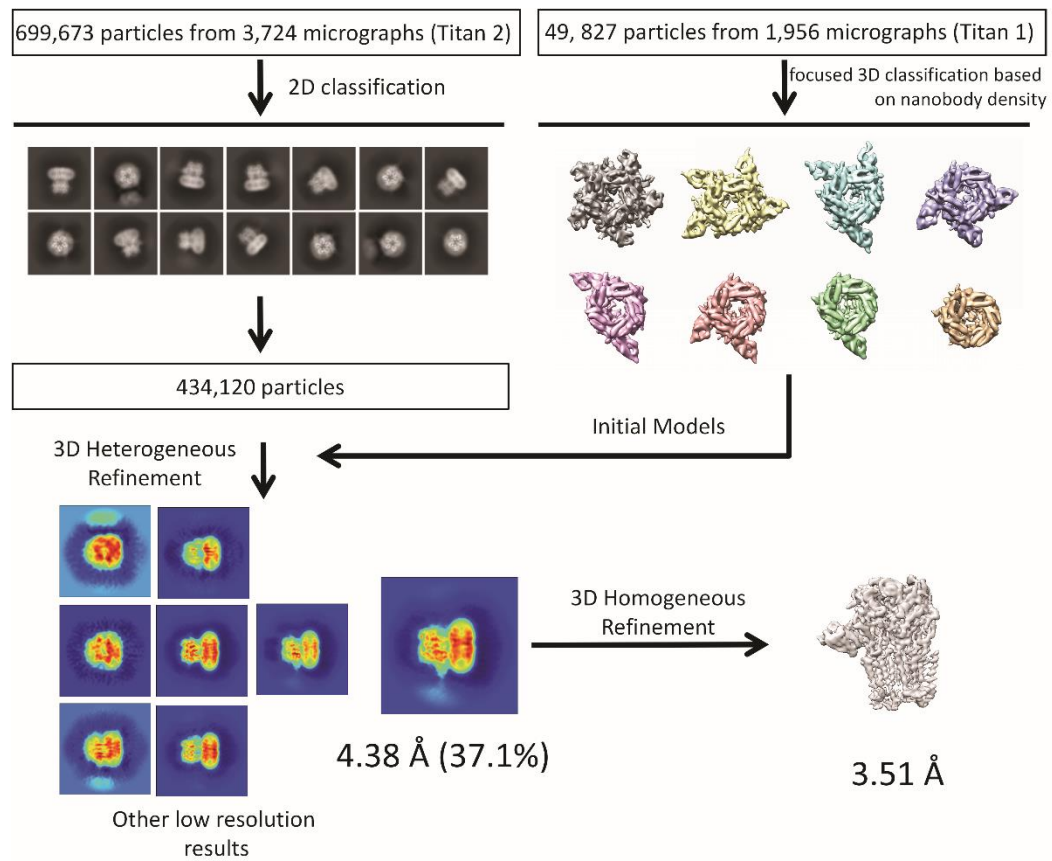
123



124

125 Figure S4. Cryo-EM map at 3σ contour level showing the N-linked glycan at Asn 205
126 of α subunit.

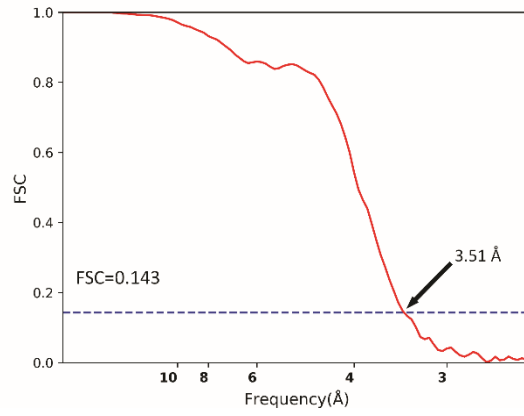
127



128

129 Figure S5. Flow chart of cryo-EM data processing

130



131

132 Figure S6. “Gold-standard” FSC coefficient curve of the final reconstruction

133